Available online at www.sciencedirect.com
SCIENCE DIRECT®
Pergamon
Acta Materialia 51 (2003) 6453–6464
Acta MATERIALIA
www.actamat-journals.com

Neutron diffraction study of stress-induced martensitic transformation and variant change in Fe–Pd

E.C. Oliver [a,b,*], T. Mori [a,b], M.R. Daymond [a], P.J. Withers [b]

[a] *ISIS Facility, Rutherford Appleton Laboratory, Chilton, Didcot, OX11 0QX, UK*
[b] *Manchester Materials Science Centre, University of Manchester and UMIST, Grosvenor Street, Manchester, M1 7HS, UK*

Received 18 March 2003; received in revised form 13 August 2003; accepted 15 August 2003

Abstract

Neutron diffraction spectra have been recorded in situ during tensile testing of polycrystalline Fe–30.5 at % Pd at a range of temperatures, in order to investigate stress-induced martensitic transformation and variant changes. The selective transformation of preferentially oriented austenite grains and martensite variants is identified and related to elasticity-based theory. Rietveld refinement is applied to determine the variation of elastic stiffness with temperature, revealing a significant increase in stiffness upon transformation to the martensite phase, in contrast to macroscopic measurements.

Keywords: Fe–Pd; Shape memory alloys (SMA); Martensitic phase transformation; Neutron diffraction; Residual stresses

1. Introduction

Considerable interest has recently been directed towards a range of ferromagnetic shape memory alloys, in which the shape memory effect may be induced not only thermally, but also magnetically. The magnetically-induced effect makes them attractive for a range of actuator applications. Among these alloys, the Fe–Pd system is of particular interest, offering potential benefits including large magnetisation, easy control of the M_s temperature by alloy composition, and a notably low elastic stiffness [1–3].

These Fe–Pd alloys exhibit a martensitic transformation from an fcc to fct crystal structure [1,2]. The thermally induced transformation in polycrystalline Fe–Pd has been investigated experimentally using optical and electron microscopy [4–6] and X-ray diffraction [1,2]. However, relatively little work has been carried out studying the martensite structure produced under applied stress. This is of interest, since under an applied stress, certain martensite orientations (variants) will preferentially form, resulting in a different structure to that induced thermally. Moreover, work is also required to examine the variant changes which occur when stress is applied to existing martensite. Conversion between variants involves the dissipative process

* Corresponding author. Tel.: +44-1235-445718; fax: +44-1235-445720.
E-mail address: e.c.oliver@rl.ac.uk (E.C. Oliver).

1359-6454/$30.00
doi:10.1016/j.actamat.2003.08.017

of interface movement; mechanical testing combined with observation of orientation changes provides a method of investigating the extent of energy dissipation. This information is relevant to both the conventional shape memory effect and the magnetic effect, which originates from magnetically-induced variant changes [7].

Neutron diffraction provides an excellent method to investigate both stress-induced transformation and variant change. While the techniques are similar, neutron diffraction offers major advantages over conventional X-ray diffraction because the penetration depth of neutrons is far greater than that of laboratory X-rays (respectively, ~10 mm and ~10 μm in iron for neutrons and X-rays of similar wavelength [8]), thus allowing bulk rather than surface properties to be probed. Further, neutron diffraction is also more appropriate than synchrotron X-ray diffraction for materials with large grain sizes, as is typical for Fe–Pd alloys, because a scattering volume of several cubic millimetres may be used in order to sample a representative grain population. There now exist dedicated engineering instruments at neutron sources, equipped with online loading rigs [9]. By carrying out in situ loading experiments, changes in crystal structure, texture and internal stress may be followed. This paper reports an application of this technique to the study of the martensitic transformation in an Fe–Pd alloy. While neutron diffraction studies of other shape memory alloys have been reported previously [10–12], the crystallography of the martensitic transformation in Fe–Pd is appealing simple, facilitating a straightforward analysis and leading to greater insights into the transformation process.

2. Martensite structure

A typical optical micrograph of polycrystalline Fe–Pd in the fully martensitic state is shown in Fig. 1. The martensite structure, observed using optical and electron microscopy, has been analysed on the basis of elasticity theory [6]. We summarise here some key points, with regard to the motivations for the present study.

Due to the higher symmetry of the parent austenite phase, the martensitic daughter structure can form with a number of different orientations or variants. One of the motivations for the present study is to identify the preferential formation of certain variants under applied stress. Although the formation of certain variants has been observed metallographically, no in situ diffraction study has yet been attempted in order to identify their orientation.

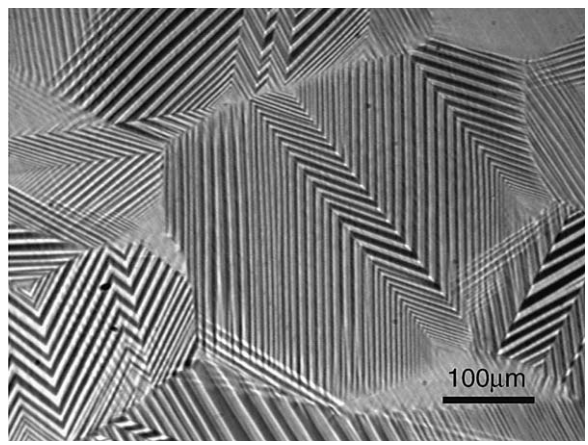

Fig. 1. Optical micrograph of martensite in polycrystalline Fe-30.5 at % Pd showing, to the right of center, a former austenite grain containing three former austenite twin boundaries.

For Fe–Pd, there are three Bain correspondence variants (BCVs), denoted BCV(1), BCV(2) and BCV(3), where the index refers to the austenite axis to which the martensite *c*-axis lies parallel. For example, BCV(1) is the variant in which the *c*-axis lies parallel to the austenite 1-axis, [1 0 0].

The stress-free transformation strain of BCV(1) is written as

$$\varepsilon^{\mathrm{T}}(1) = \begin{pmatrix} \varepsilon_c & 0 & 0 \\ 0 & \varepsilon_a & 0 \\ 0 & 0 & \varepsilon_a \end{pmatrix}. \quad (1)$$

Here,

$$\varepsilon_a = (a - a_0)/a_0, \ \varepsilon_c = (c - a_0)/a_0, \quad (2)$$

where a_0 is the stress-free lattice parameter of austenite and a and c are, respectively, the stress-free

lattice parameters of the *a*-axes and the *c*-axis of martensite. The strain components satisfy

$$\varepsilon_a > 0,\ \varepsilon_c < 0,\ \varepsilon_a + \varepsilon_c < 0 \tag{3}$$

[2]. The transformation strains of BCV(2) and BCV(3) are obtained by permuting the diagonal components in (1).

When the austenite phase is cooled below the martensite start temperature, M_s, martensite plates begin to form within the austenite matrix. The structure of a martensite plate consists of fine twins of two of the three BCVs, joined along stress-free {1 1 0} interfaces [6]. For example, a plate consisting of BCV(1) and BCV(2) has average transformation strain

$$\bar{\varepsilon}^{\mathrm{T}} = f\varepsilon^{\mathrm{T}}(1) + (1-f)\varepsilon^{\mathrm{T}}(2) \tag{4}$$

$$= \begin{pmatrix} \varepsilon_a - f(\varepsilon_a - \varepsilon_c) & 0 & 0 \\ 0 & \varepsilon_c + f(\varepsilon_a - \varepsilon_c) & 0 \\ 0 & 0 & \varepsilon_a \end{pmatrix},$$

where f is the volume fraction of BCV(1). Eq. (4) is written using an infinitesimal deformation approach [13], since the magnitudes of ε_a and ε_c are small [2]. Using this approach, it may be shown that if the habit plane has a certain orientation and f takes the value $\varepsilon_a/(\varepsilon_a - \varepsilon_c)$ or $-\varepsilon_c/(\varepsilon_a - \varepsilon_c)$, the plate is formed without the generation of internal stress [6]. Since there are three possible combinations of two BCVs, and two solutions of f for each, there exist a total of six possible variants of stress-free plates with different transformation strains (in addition, there are two solutions for the habit plane orientation of each variant, but this is not relevant to the discussion below).

Let us consider stress-induced transformation in a single austenite crystallite under uniaxial tensile loading, with the tensile axis lying inside the standard stereographic triangle of [0 0 1]–[1 0 1]–[1 1 1]. In order to maximise elongation along the tensile axis, the applied stress favours the formation of BCV(2) over BCV(1), and both over BCV(3). Thus, of the six possible types of twinned plate, that composed in the majority of BCV(2) with a minority of BCV(1) is most favoured by the applied stress. Considering (3), this has $f = \varepsilon_a/(\varepsilon_a - \varepsilon_c)$ and, from (4), its average stress-free transformation strain is

$$\bar{\varepsilon}^{\mathrm{T}} = \begin{pmatrix} 0 & 0 & 0 \\ 0 & \varepsilon_a + \varepsilon_c & 0 \\ 0 & 0 & \varepsilon_a \end{pmatrix}. \tag{5}$$

The elongation along the tensile axis is maximised if the tensile direction is parallel to [0 0 1]. Thus, in an austenite polycrystal, neglecting the constraint of surrounding grains, stress-induced transformation is most favoured in those grains oriented with the tensile axis parallel to an ⟨0 0 1⟩ direction. Experimental verification of this prediction is one motivation for the present study.

We note in passing that a strict energetics analysis demonstrates that the structure of a plate formed under applied stress would be expected to deviate somewhat from that which gives rise to zero internal stress, with f varying accordingly [14]. However, in the temperature range examined in the present study, the expected deviation of f is small, and can be neglected.

When cooled into the fully martensitic state in the absence of applied stress, each original austenite grain develops a compound twin martensite structure, consisting of alternating lamellar plates. These are seen in the optical micrograph of Fig. 1 as alternating bright and dark lines of surface relief. Each plate itself consists of fine twins (not observable using optical microscopy) of two BCVs, joined along stress-free {1 1 0} interfaces, as described above. The two BCVs constituting a plate are also twin-related along {1 1 0} interfaces to those in the adjacent plate [6]. When formed by simple cooling, the volume fraction of each BCV within a former austenite grain is equal to 1/3. This minimises the generation of internal stress, since the average transformation strain is purely dilatational, and the same for all grains [6].

Consider again, however, the effect of applying uniaxial tensile stress along an axis which lies within the standard triangle, relative to the crystal axes of a particular grain. Since BCV(2) is favoured by the applied stress, the fraction of this BCV within the grain is expected to grow at the

expense of the other variants, via the movement of twin boundaries. This is an important origin of the shape memory effect. The variant change should be detectable by changes in the neutron diffraction spectrum, and its observation is another motivation for the present study.

Finally, the present study also investigates the elastic stiffness of the Fe–Pd system. Previous stiffness measurements on Fe–Pd have used strain gauges to monitor the macroscopic strain [5]. However, this method does not allow a separation of elastic strain and strain due to transformation or variant change. Diffraction monitors lattice spacing and therefore provides a direct measurement of elastic strain, allowing the determination of the true elastic stiffness.

3. Experimental

After an extended dwell at 1250 °C, a 25 mm thick ingot of polycrystalline Fe–30.5 at % Pd alloy was free forged between 900 and 1000 °C in several passes into a rod of diameter 6 mm. Intermediate annealing was employed to avoid cracking. A tensile specimen was machined with gauge length 50 mm, diameter 4.5 mm, and threaded ends. The specimen was quenched from 1050 °C into water.

Neutron diffraction spectra were recorded in situ during uniaxial tensile loading, using the ENGIN engineering instrument at the ISIS spallation neutron source, as described in detail in [15]. The instrument has two detector banks which measure time-resolved spectra at fixed horizontal scattering angles of ±90°. Thus, the scattering vectors are fixed at ±45° to the incident beam, and each *hkl* reflection is produced by a different family of appropriately oriented grains. The load axis was aligned horizontally at 45° to the incident beam, such that the scattering vectors were aligned axially and transversely to the applied load. With reference to this geometry, the diffraction spectra recorded in the two detector banks are hereafter denoted as axial and transverse spectra. Incident slits and radial collimators defined a scattering volume of approximately $5 \times 5 \times 1.5$ mm^3. Diffraction spectra were acquired using count times of approximately 45 min. The applied stress and temperature were held constant during each measurement. The specimen was both mechanically loaded at a range of temperatures between −1 and 30 °C, and thermally loaded in the absence of applied stress. Between tensile tests, the specimen was annealed for 30 min at 40 °C in order to return the material to the fully austenitic state. The test temperature was maintained via conduction through the specimen grips, through which temperature-controlled oil was pumped. The temperature was monitored using a thermocouple attached to the sample surface in the vicinity of the scattering volume. Temperature stability of ±1 °C was achieved. The specimen strain was monitored using an extensometer, except during the test at −1 °C, when strain was monitored using crosshead displacement alone, in order to avoid temperature fluctuations introduced by contact of the extensometer with the specimen. The macroscopic stress–strain response of the specimen at −1 °C was however recorded using an extensometer after completion of the neutron diffraction experiment.

4. Results and discussion

By observing the evolution of the diffraction spectra during cooling and heating, the temperatures at which martensite starts to form during cooling, M_s, and the reverse transformation finishes during heating, A_f, were determined, respectively, as approximately 16 and 17 °C. That is, the alloy exhibits low temperature hysteresis.

The following notation and terminology is used in the remainder of this paper. Austenite and martensite diffraction peaks are referred to as $h\ k\ l_a$ and $h\ k\ l_m$, respectively, where $h\ k\ l$ are the Miller indices. The term *h k l*-type refers to the family of austenite grains in which a $\langle h\ k\ l \rangle$ direction lies parallel to the tensile axis.

4.1. Macroscopic response

The macroscopic stress–strain response acquired during the neutron diffraction test at 24 °C is shown in Fig. 2a. At this temperature, the material was initially fully austenitic. Plateaus are evident

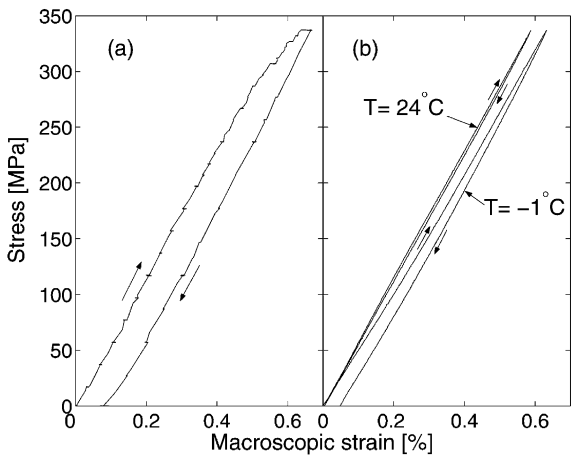

Fig. 2. Macroscopic stress-strain response: (a) at 24 °C, recorded during neutron data collection; (b) recorded on same specimen after neutron data collection, strain rate 1.2×10^{-5} s^{-1}. Arrows indicate the direction of loading.

where the stress was held constant during data collection. Prior to this test, the specimen had been loaded to 280 MPa at −1 °C. The loading response is approximately linear up to this stress, but at higher stresses, the response deviates towards greater strain. The deviations are partly due to a small amount of creep which occurred during the dwells at constant stress. As seen from the unloading curve, approximately 0.1% strain was not recovered after unloading; nor was it recovered during the subsequent anneal. This suggests that the unrecovered strain was due to slip plasticity rather than martensitic transformation. To assess this, a second tensile test at 24 °C was performed after the neutron diffraction tests. The strain developed in this test was fully recovered upon unloading (Fig. 2b), indicating that the material had work hardened and the unrecovered strain in the former test was indeed developed by slip. Also shown in Fig. 2b is the response measured after the neutron diffraction tests at −1 °C, at which temperature the material was fully martensitic throughout loading. The initial slope is slightly lower than that measured at 24 °C. Unlike at the higher temperature, at −1 °C approximately 0.05% strain remained unrecovered after unloading, even though the earlier work hardening is expected to have prevented further slip. This strain was, however, recovered by subsequent annealing at 40 °C and may thus be attributed to martensitic variant change.

4.2. Thermal loading

Fig. 3a shows the initial, fully austenitic axial diffraction spectrum, recorded at 24 °C. Fig. 3b shows the corresponding martensite spectrum obtained by cooling to −1 °C. All austenite reflections in the spectral region shown have Miller indices of the general form hhk_a. It can be seen that in general the transformation causes such a reflection to split into the two martensite reflections with indices hhk_m and khh_m, lying either side of the parent austenite reflection. The reflection with the larger d-spacing depends on whether $h > k$. Since the transformation strain is small, all three reflections have similar d-spacings. For example, $2\,0\,0_a$ splits into the $2\,0\,0_m$ and $0\,0\,2_m$ reflections. Similarly, $2\,2\,0_a$ splits into $2\,2\,0_m$ and $0\,2\,2_m$. Due to symmetry, there is a single $1\,1\,1_m$ peak. The relative intensities of the austenite peaks are similar to those expected for a powder, indicating that the grains are approximately randomly oriented. For time-of-flight neutron diffraction, scattered intensity is proportional λ^4, where λ is the wavelength and, thus, to d^4, where d is the lattice spacing

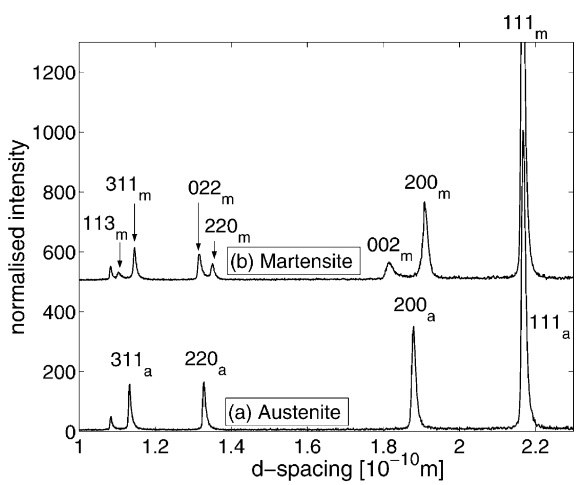

Fig. 3. (a) Initial austenite spectrum (axial) at 24 °C; (b) corresponding martensite spectrum obtained by cooling to −1 °C. The martensite curve has been displaced vertically for clarity.

(since $d \propto \lambda$) [16]. In the martensite spectrum, after correcting for this dependence, the ratio of the $2\,0\,0_m$ to $0\,0\,2_m$ peak intensities and that of the $0\,2\,2_m$ to $2\,2\,0_m$ peak intensities are both close to the ideal 2:1 ratio which would be expected if all former austenite grains contained equal proportions of each BCV.

Fig. 4 shows the lattice parameters of martensite (a and c) and austenite (a_0) between -1 and 30 °C, as determined by Rietveld refinement of the diffraction spectra, using the GSAS package [16]. Datapoints joined by continuous lines represent values determined in the absence of applied stress. Linearly extrapolating these data to M_s, the lattice parameters determined at this temperature are $a_0 = 0.3752$, $a = 0.3797$ and $c = 0.3668$ nm, giving transformation strain components of $\varepsilon_a = 1.20 \times 10^{-2}$ and $\varepsilon_c = -2.24 \times 10^{-2}$. These values confirm (3), ensuring that martensite plates free of internal stress can potentially exist [13]. As reported by other authors [1,2], the ratio c/a decreases as the temperature decreases below M_s. However, Fig. 4 certainly demonstrates a jump in the lattice parameters at the transition temperature, indicating that the transformation is of the first order, rather than a pseudo second order transformation, as it has often been described in the past [17].

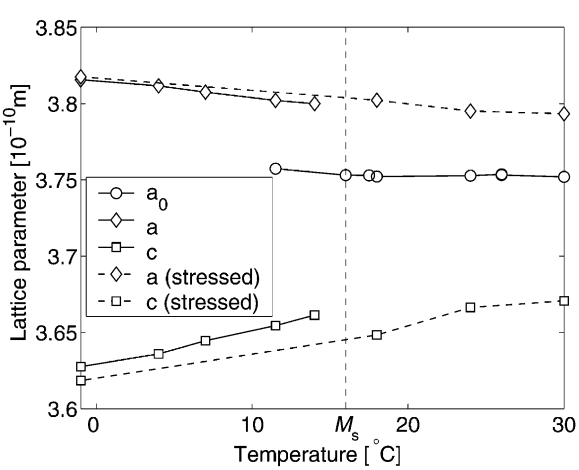

Fig. 4. Lattice parameters of austenite and martensite versus temperature, determined by Rietveld refinement of the diffraction spectra. Continuous lines: measured in the absence of applied stress; dashed lines: determined from transverse spectra under applied stress (280 MPa for the points measured below M_s, 340 MPa for all other points). Statistical fit uncertainties from the Rietveld refinements are too small to represent. The martensite start temperature M_s is indicated by a dashed vertical line.

Martensite lattice parameters can be determined for temperatures above M_s from the spectra recorded under applied stress, when stress-induced martensite was present. The points joined by dashed lines in Fig. 4 represent values measured under stress. These are determined from the transverse rather than axial spectra, since this provides a more useful comparison with the stress-free data for two reasons. Firstly, as discussed below, the preferential selection of martensite variants causes certain peaks to be absent in the axial spectra. Secondly, while elastic strains may significantly alter the lattice parameters determined from the axial spectra acquired under stress, this influence is less significant in the transverse direction, which is affected only by Poisson contraction. All measurements in this dataset were recorded under a tensile stress of 340 MPa, except for the points below M_s which were measured at a slightly lower tensile stress of 280 MPa (assuming a Young's modulus at -1 °C of 140 GPa—as presented in Section 4.5—and a Poisson's ratio of 0.3, the difference of 60 MPa alters the Poisson contraction of the lattice parameters by approximately 5×10^{-4} Å, which is smaller than the symbol size used in Fig. 4 and may be safely neglected). The dashed lines further demonstrate that the martensite lattice parameters do not converge to the austenite lattice parameter with increasing temperature, supporting the argument that the transformation is not pseudo second order. Comparing the dashed and continuous lines, two effects are evident. Firstly, Poisson contraction due to the applied stress results in a systematic lowering of the lattice parameters. This, however, is coupled with an increased splitting of the a and c lattice parameters. Counter-intuitively, this results in the a parameter measured transverse to the loading axis increasing when a tensile stress is applied. Thus, the splitting cannot be attributed simply to elastic anisotropy. The effect may possibly be related to stabilisation of martensite by the applied stress, but in order to understand this, a full explanation is first required for the variation of c/a with temperature.

4.3. Stress-induced transformation

Fig. 5 shows the spectra observed at 24 °C under a tensile stress of 340 MPa. In the axial spectrum (Fig. 5a), the 2 0 0_a reflection is weak and visible only in the shoulder of the strong 2 0 0_m reflection. The 0 0 2_m reflection is undetectable. This demonstrates that austenite grains with <1 0 0> aligned parallel to the tensile axis transform preferentially to those martensite variants whose *a*-axes are parallel to the tensile direction, confirming the prediction from our argument in Section 2. In the corresponding region of the transverse spectrum (Fig. 5b), all three reflections are present. Interpretation of the relative peak intensities in the transverse spectrum is not so straightforward, since a grain with certain crystallographic direction pointing in the transverse direction may have any of a range of directions lying parallel to the tensile axis. Nevertheless, it is still possible to gain supporting evidence from the transverse spectra. For example, austenite grains with ⟨1 0 0⟩ lying transversely may have directions between ⟨1 0 0⟩ and ⟨1 1 0⟩ oriented axially. Since the weakening of the axial 2 0 0_a reflection is due to a large degree of transformation in grains with ⟨1 0 0⟩ aligned axially, the fact that the same reflection remains relatively intense in the transverse spectrum indicates that other grains in which ⟨1 0 0⟩ lies transversely—i.e. those in which the tensile axis lies closer to ⟨1 1 0⟩—are less favoured for transformation by the applied stress, remaining untransformed.

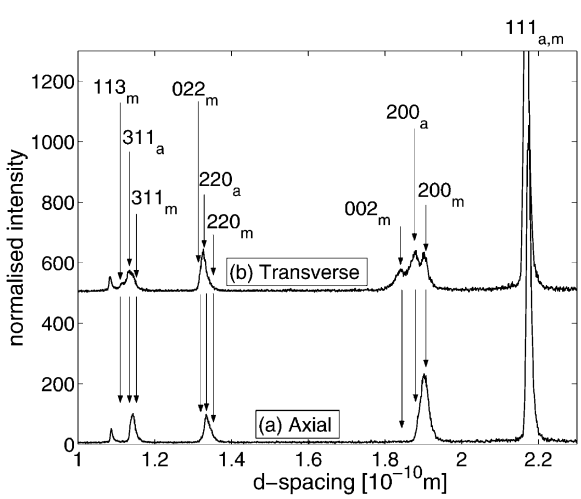

Fig. 5. (a) Axial and (b) transverse diffraction spectra recorded at a temperature of 24 °C under a tensile stress of 340 MPa. The transverse spectrum has been displaced vertically for clarity.

The preferential selection of martensite variants is also evident in the vicinity of the 3 1 1_a reflection. In the transverse spectrum, both the 3 1 1_m and 1 1 3_m peaks are visible, but the latter is absent in the axial spectrum. Again, this indicates that those variants which result in elongation along the tensile axis are preferentially formed. Close inspection of the axial spectrum evolution in the vicinity of the 2 2 0_a reflection reveals however that both the 2 2 0_m and 0 2 2_m peaks develop, even though the presence of the latter indicates the formation of a variant which contracts along the tensile axis. This is reasonable since, as discussed in Section 2, a martensite plate must be formed of two of the three available BCVs in order to minimise the generation of internal stress. With this austenite grain orientation, two of the three possible BCVs are symmetry related with respect to the tensile axis and both give rise to contraction; thus necessarily one of the two BCVs in the plate causes contraction. However, taken in combination with the elongation of the majority variant, the overall transformation strain of the combined plate remains elongational along the tensile axis, and thus the plate formation remains favoured by the applied stress.

Fig. 6 shows the variation with applied stress of the axial spectrum integrated intensities of the 2 0 0_a, 3 1 1_a and 2 2 0_a reflections, and the corresponding martensite reflections. The intensities are scaled by a factor of d^4, to account for the variation of scattered intensity with lattice spacing. Moreover, the intensities of related austenite and martensite peaks are normalised by the maximum intensity recorded for the austenite reflection. For each reflection set, the reduction in austenite reflection intensity is accompanied by an approximately equal increase in martensite reflection intensity. At a given applied stress, the fractional reduction in intensity of the austenite reflections increases in the order 2 2 $0_a \rightarrow 3\ 1\ 1_a \rightarrow 2\ 0\ 0_a$. This indicates that the tensile stress induces transformation most readily in 1 0 0-type grains, i.e. those

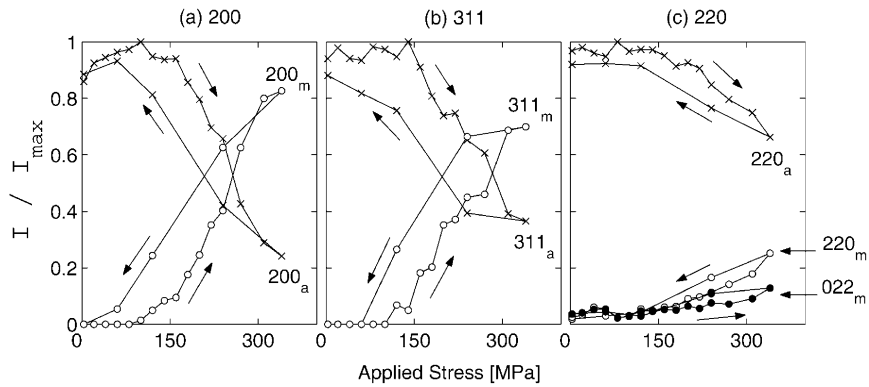

Fig. 6. Variation of axial spectrum integrated peak intensities with applied stress, during stress-induced transformation at 24 °C. Crosses—austenite reflections; circles—martensite reflections with same Miller indices, as labelled for each plot. Intensities are scaled by the fourth power of the *d*-spacing, and normalised with respect to the maximum intensity of the appropriate austenite reflection. Arrows indicate the loading and unloading curves.

oriented such that a ⟨1 0 0⟩ direction lies parallel to the tensile axis. Transformation is less favoured as the angle between ⟨1 0 0⟩ and the tensile axis increases. This trend concurs with the prediction given in Section 2: the formation of a martensite plate causes greatest elongation along a ⟨1 0 0⟩ direction, as is clear from Eq. (5); thus the external potential energy is most greatly reduced by plate formation in a 1 0 0-type grain.

Although the trend of selective transformation is clearly evident, quantitative analysis is rather involved in the case of a polycrystal, due to the constraint imposed by surrounding grains and the resulting build up of internal stress. This constraint acts against the trend of selective transformation of preferentially oriented crystallites, since the elongation developed in transformed grains gives rise to axially compressive internal stresses in these grains, balanced by tensile internal stresses in untransformed grains. Thus, the internal stress acts to promote the transformation of less favourably oriented grains. This is analogous to the case of polycrystalline plasticity. For example, consider the case of an ideally plastic, elastically isotropic, randomly oriented fcc polycrystal, as analysed by Budiansky and Wu [18]. The ratio of the maximum to minimum Schmid factors in fcc single crystals is 1.84. However, the limiting stress which causes yielding in all grains of the ideally plastic polycrystal is only 1.54 times the initial yield stress. That is, the internal stress caused by the yielding of favourably oriented grains augments the stress acting upon less favourably oriented grains.

As noted above, both the $2\,2\,0_m$ and $0\,2\,2_m$ martensite reflections are evident in the axial spectra. The intensities of both of these reflections are plotted in Fig. 6. At the maximum applied stress, the ratio of the $2\,2\,0_m$ to total martensite intensity is 0.66. This is in very good agreement with the value of 0.65 calculated for Fe–30.5at% Pd for the majority BCV fraction in a martensite plate which is free of internal stress [14], supporting the expectation given in Section 2 that tensile stress does not strongly alter the twin structure of martensite plates.

All the curves plotted in Fig. 6 exhibit hysteresis but in each case the reverse transformation is almost completed at the end of unloading. This demonstrates the reversibility of the stress-induced transformation. This is to be expected, since the deformation temperature of 24 °C is sufficiently higher than A_f which, as noted earlier, is only approximately 1 °C higher than M_s. Furthermore, the observed near completion of the reverse transformation upon unloading is in accordance with the observation made in Section 4.1 that the tensile strain is fully recoverable when slip plasticity does not occur.

Similar changes in the diffraction spectra were observed during tensile tests performed at 18 and

30 °C. The stress at which transformation is first observed is expected to increase with temperature above M_s, as the austenite phase is stabilised relative to martensite. The rate of increase of onset stress with temperature is also expected to rise. For 1 0 0-type grains—i.e. optimally oriented for transformation, as discussed above—the onset stresses were determined as approximately 40, 120 and 140 MPa at 16, 24 and 30 °C. This qualitatively confirms the first of the above expectations, but not the second. It is likely that the observed onset stresses are influenced by the sample history, since the same sample was used for all tests due to the limited amount of available material. The test at −1 °C was performed first, followed by the tests at 24, 18 and 30 °C, in that order. In each test, a small amount of non-recoverable strain was generated (less than 0.3% in total after all tests) which, as discussed in Section 4.1 and by other authors [5], can be attributed to slip plasticity, since it develops even if the reverse transformation is complete. The generation of intergranular stresses associated with this plasticity is evident from the Rietveld refinements of the spectra recorded in the absence of applied stress. Since the refinement does not account for grain orientation dependent deviations from the average lattice parameter, differences between the Rietveld-determined and real peak positions can be attributed to the generation of intergranular stresses. Interpreting the refinements in this way reveals that, as previously reported in fcc steels [19], the slip plasticity causes tensile residual stress in 1 0 0-type grains, and that the magnitude of this residual stress continues to increase throughout the series of tests. This tensile residual stress will act to promote transformation in these grains, suggesting an explanation for why the onset stress measured at 30 °C appears to be suppressed relative to that measured earlier at 24 °C. More experimentation—using virgin samples and a wider temperature range—is therefore required to fully analyse the temperature dependence of the onset stress.

4.4. Stress-induced variant change

The material was fully martensitic throughout the loading test conducted at −1 °C. Fig. 7 compares the axial diffraction spectrum recorded at this temperature under an applied stress of 5MPa (introduced solely to remove slack from the sample/grip system) and under an applied stress of 280MPa. Reorientation of the martensite structure is evident from changes in the diffraction peak intensities. In general, among $h\ h\ k_m$–$k\ h\ h_m$ pairs, the intensity of the reflection with smaller d-spacing falls with tensile stress, and the intensity of the reflection with larger d-spacing increases. This indicates variant change to those variants which have a greater elongation in the direction of the tensile stress. For example, the $0\ 0\ 2_m$ peak weakens as the $2\ 0\ 0_m$ peak grows, indicating that BCVs with the c-axis aligned parallel to the tensile axis are converted to those with an a-axis pointing in this direction. This change results in elongation parallel to the tensile axis and is thus favoured by the applied stress.

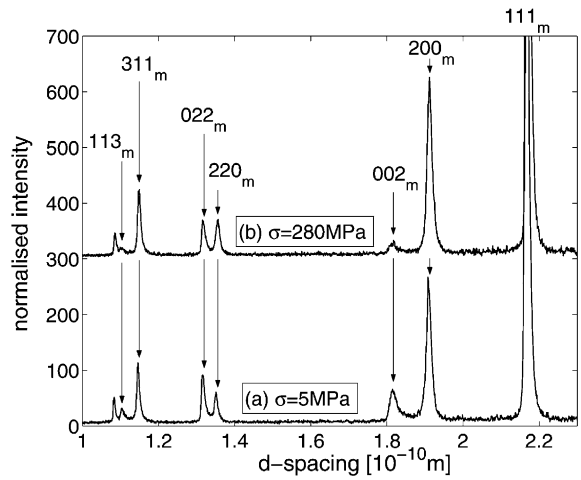

Fig. 7. Axial diffraction spectra recorded at a temperature of −1 °C and applied tensile stress σ of (a) 5 MPa; (b) 280 MPa. The latter spectrum has been displaced vertically for clarity.

The variation of axial diffraction peak intensities with applied stress is shown in Fig. 8. Significant intensity changes are evident even in the spectra recorded after the first applied stress increment (to 70 MPa). This suggests that the frictional stress—which must be overcome to nucleate the dislocations required for BCV interface movement—is somewhat smaller than this. It also suggests an explanation for the drop in the apparent macro-

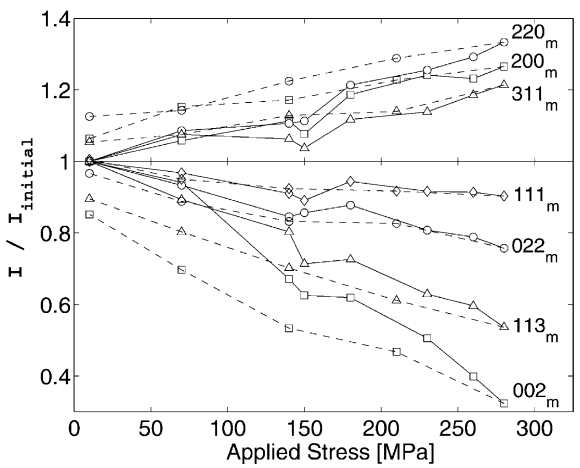

Fig. 8. Variation of axial martensite spectrum integrated peak intensities with applied stress, during tensile straining at −1 °C. The intensities are normalised with respect to the initial intensities. The loading and unloading curves are represented by continuous and dashed lines, respectively.

scopic stiffness when the temperature is reduced below M_s, as noted in Section 4.1 and reported elsewhere [5]. That is, variant change is active even at small applied stresses, giving rise to non-elastic strains and reducing the apparent stiffness.

The orientation dependence of the variant changes is very clear and follows the same trend observed for the stress-induced phase transformation. Of the reflections which lose intensity, at a given applied stress the relative reduction increases in the order $0\,2\,2_m \rightarrow 1\,1\,3_m \rightarrow 0\,0\,2_m$. This indicates that BCVs with [0 0 1] aligned parallel to the tensile axis most readily change orientation under the application of tensile stress. As in the case of the phase transformation, this is because the elongation resulting from the change is maximised for this orientation.

Since all BCVs have the same transformation strain resolved along the austenite [1 1 1] direction, a large intensity change due to variant re-orientation is not expected for the $1\,1\,1_m$ reflection. Of all the reflections considered, the fractional intensity change is indeed smallest for $1\,1\,1_m$. However, a significant reduction of 11% is still observed at the maximum applied stress. Variant change does in fact lead to a slight tensile elongation when the tensile axis is aligned parallel to the martensite (1 1 1) normal, since this direction does not lie exactly parallel to austenite [1 1 1]. The resulting change in the direction of the normal of approximately 2° may be sufficient that the variant no longer contributes to the {1 1 1} reflection. However, since the elongation is only approximately 2% of that achieved in a BCV oriented with [0 0 1] parallel to the tensile axis, the magnitude of the $1\,1\,1_m$ intensity reduction remains somewhat surprising.

Of the reflections which increase in intensity, at a given applied stress the relative intensity gains increase in the order $3\,1\,1_m \rightarrow 2\,0\,0_m \rightarrow 2\,2\,0_m$. The order is not the same as for the corresponding intensity losses due to the influence of multiplicity. That is, in 2 0 0- and 3 1 1-type grains, only one of the three BCVs can elongate by changing into another variant, while in 2 2 0-type grains, two of the three can do so. Thus, assuming all former austenite grains initially contain equal proportions of each BCV, variant changes can cause the intensities of the $2\,0\,0_m$ and $3\,1\,1_m$ reflections to grow by a maximum factor of 1.5, but that of $2\,2\,0_m$ by a maximum factor of 3. Taking this into account, it is seen that the intensity gains in fact indicate that the greatest extent of variant change occurs in the 2 0 0-type grains, in agreement with the trend seen from the intensity losses.

Upon unloading, the axial reflection intensities return to within 15% of their initial values, indicating the reversal of the variant changes. Since no chemical energy change is involved, this reversal must be driven by internal stress, due to the incompatibilities generated between differently oriented grains. For example, the inability of 1 1 1-type grains to elongate significantly by variant change results in axially tensile internal stress in such grains, balanced by axially compressive internal stress in other grains, driving the reverse changes when the external load is removed. The fact that the intensities do not fully return to their initial values supports the point made in Section 4.1, that some macroscopic strain remains after unloading due to variant change.

Although not presented here due to the limitation of space, the transverse spectra acquired during deformation at −1 °C provide supplementary

information which supports the conclusions drawn from analysis of the axial spectra.

4.5. Elastic stiffness

Since Rietveld refinement provides a method of elastic strain determination [20], it can be applied to give a measure of Young's modulus which is not partially obscured by the development of non-elastic strain. Fig. 9 shows the variation of Young's modulus with temperature, determined by fitting straight lines to the initial slopes (prior to the onset of stress-induced transformation) of the curves of Rietveld-determined axial elastic strain versus applied stress. Also shown is the macroscopic stiffness determined using the extensometer. Above M_s, the Rietveld-determined estimates of Young's modulus are slightly higher than the corresponding macroscopic values, suggesting the macroscopic strain may include a small amount of transformation strain even at low stresses. The values are in reasonable agreement with those determined in a recent study by Kato, et al. using a strain gauge method [4,5]. The Young's modulus falls with reducing temperature due to lattice softening, to a value of approximately 50 GPa at M_s. Below M_s, the Rietveld-determined stiffness rises sharply, to 140 GPa at −1 °C. This indicates that the lattice softens as the transformation temperature is approached from either above or below, as expected from the physical origin of the phenomenon, i.e. the broadening of the minimum of the free energy-atomic displacement curve near the transformation temperature [21]. However, the macroscopic stiffness does not follow the sharp rise in the Rietveld-determined stiffness: at −1 °C it is only 50 GPa. Kato et al. in fact reported a significant drop in the macroscopic stiffness below M_s. These observations suggest that even at low stresses, much of the macroscopic strain is due to variant change, in accordance with the intensity changes observed at small applied stresses in Fig. 8. Since the elastic stiffness is a fundamental property required for the basic understanding and application of the material, it would be beneficial to apply neutron diffraction to a more comprehensive characterization of its variation with temperature.

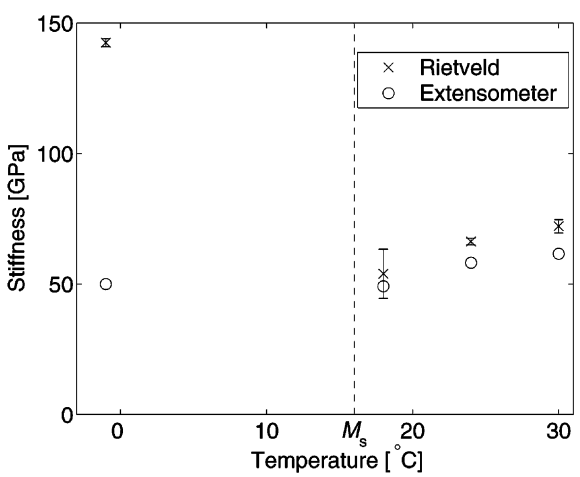

Fig. 9. Temperature dependence of Young's modulus, determined by Rietveld refinement, and macroscopic stiffness, determined using an extensometer, of Fe–30.5 at % Pd. Error bars on the Rietveld-determined datapoints represent statistical uncertainties in the fits to the stress–elastic strain responses. Statistical uncertainties in slopes fitted to the macroscopic stress–strain curves are too small to represent. The martensite start temperature M_s is indicated by a dashed vertical line.

5. Conclusion

Neutron diffraction has been used to follow stress-induced martensitic transformation and variant change in a Fe–30.5 at % Pd polycrystal during tensile testing. The tests on initially austenitic material have revealed the selective formation of those martensite variants which produce the greatest elongational strain along the tensile axis. The greatest extent of transformation is achieved in austenite grains oriented with a ⟨1 0 0⟩ direction parallel to the tensile axis, since this maximises the elongational strain developed during martensite plate formation. The measurements support an elasticity-based analysis of the martensite structure. The test on initially martensitic material has demonstrated that variant changes occur even at small applied stresses, causing the macroscopic stiffness to be substantially lower than the real elastic stiffness, as determined from the diffraction data. The neutron diffraction technique has provided an effective method of separating elastic and

transformation strain, which may be applied in future to further investigate the substantial lattice softening which occurs close to the transformation temperature.

Acknowledgements

We would like to thank Dr M. Okabe and Mr S. Ueta of Daido Steel Company, Japan, for kindly producing and supplying the material for this study. Funding under EPSRC project GR/R07936 is gratefully acknowledged.

References

[1] Sohmura T, Oshima R, Fujita F. Scripta Metall 1980;14:855.
[2] Oshima R. Scripta Metall 1981;15:829.
[3] Sugiyama M, Harada S, Oshima R. Scripta Metall 1985;19:315.
[4] Kato H, Wada T, Tagawa T, Liang Y, Taya M. In: Proc 50th Anniv Jap Soc Mater Sci. 2001. p. 296.
[5] Kato H, Liang Y, Taya M. Scripta Mater 2002;46:471.
[6] Kato H, Wada T, Liang Y, Tagawa T, Taya M, Mori T. Mater Sci Eng A 2002;332:134.
[7] James R, Wuttig M. Phil Mag A 1998;77:1273.
[8] Hutchings MT, Windsor CG. Methods Exp Phy 1987;23C:405.
[9] Johnson MW, Edwards L, Withers PJ. Physica B 1997;234:1141.
[10] Vaidyanathan R, Bourke MAM, Dunand DC. Metall Mater Trans A 2001;32:777.
[11] Šittner P, Lukáš P, Neov D, Daymond MR, Novák V, Swallowe GM. Mater Sci Eng A 2002;324:225.
[12] Tomota Y, Harjo S, Lukáš P, Neov D, Šittner P. JOM-J Miner Met Mater Soc 2000;52:32.
[13] Liang Y, Kato H, Taya M, Mori T. Scripta Mater 2000;43:535.
[14] Oliver EC, Kobayashi N, Mori T, Daymond MR, Withers PJ. Scripta Mater 2003;49:1013.
[15] Daymond MR, Priesmeyer HG. Acta Mater 2001;50:1613.
[16] Larson A, von Dreele RB. GSAS—General Structure Analysis System. Tech Rep LA-UR-86-748, Los Alamos National Laboratory, Los Alamos, USA; 1994.
[17] Oshima R. Bull JIM 1989;28:493.
[18] Budiansky B, Wu TT. In: Proc Fourth US Natl Cong Appl Mech (Berkeley). New York: ASME; 1962. p. 1175.
[19] Clausen B, Lorentzen T, Bourke MAM, Daymond MR. Mater Sci Eng A 1999;259:17.
[20] Daymond MR, Bourke MAM, Von Dreele RB, Clausen B, Lorentzen T. J Appl Phys 1997;82:1554.
[21] Nakanishi N. Prog Mater Sci 1979;24:143.